Proceedings of Symposium on Microstructure and Microscopy of Magnetic Materials, May 14-15, 1998, Ames, IA, ed. by M Govindaraju, publ.. by Iowa State University

ORNL/CP-98593



# MICROSTRUCTURAL CHARACTERIZATION OF HIGH ENERGY PRODUCT Nd-Fe-B RAPIDLY SOLIDIFIED RIBBONS

J. A. Horton, M.K. Miller, L. Heatherly, J. W. Jones, K. F. Russell and V. Panchanathan*
Oak Ridge National Laboratory, Oak Ridge, TN 37831-6115
*Magnequench International, Inc. Anderson, IN 46013



## Introduction

The bonded Nd-Fe-B market has experienced the fastest growth of any permanent magnet market (1). Rapidly solidified Nd-Fe-B forms the basis for this bonded magnet industry. Rapid solidification is carried out by melt spinning, producing a highly stable and magnetically hard microstructure. The melt spun ribbons are ground into powder before being processed into bonded magnets. Of the various isotropic powders manufactured by Magnequench International (MQI), MQP-B powder has become the industry standard for multipole rings used in stepper and spindle motors (2). The continuous process and product improvements led to the development of a new powder, MQP-B+. The $B_r$ value of this powder, >8.4 kG, is higher than MQP-B and the new powder has an improved squareness of the demagnetization curve with a minimum intrinsic induction $B_d$ equal to 6 kG at a reverse field of 6kOe as compared to 4.5 kG for the original MQP-B powder. The magnetic properties are given in Table 1. A typical demagnetization curve is shown in figure 1. The specification values for the commercial version of MQP-B+ are also given in Table 1. Note that these values are given without any demag factor applied as is normally done by Magnequench for all their isotropic powders.

This study focuses on a microstructural analysis of this melt spun ribbon using transmission and scanning electron microscopy (TEM and SEM), atom probe field ion microscopy (APFIM) and Auger electron spectroscopy (AES). Atom probe and AES are both relatively unused techniques in the study of the microstructure of magnetic materials and were used here to gain some information on the compositions and thickness of any grain boundary phase. AES has the advantage of simple specimen preparation, the specimen is broken inside the UHV analy-

## DISCLAIMER

TABLE 1. Magnetic Properties of the Analyzed Ribbons

| | No Demag Factor | With 0.333 Demag Factor |
|---|---|---|
| ***Experimental Values*** | | |
| $B_r$, kG | 8.5 | 9.2 |
| Hci, kOe | 10.0 | 10.0 |
| $BH_{max}$, MGOe | 14.7 | 16.5 |
| ***Specification Values*** | | |
| $B_r$, kG | >8.4 | |
| Hci, kOe | 9.0 to 10.5 | |
| $B_d$ (min), kG | 6.0 (reverse field of 6 kOe) | |

sis chamber and immediately analyzed. Previous studies have shown that the fracture even in the small grained Magnequench material is intergranular (3). The atom probe has the advantage of a relatively direct and therefore accurate compositional measurement of very small phases. The small grain sizes, 30 to 40 nm, present in the melt spun ribbons and presumably thin grain boundary phases are a good match to the scale examined by APFIM (4).

## Experimental Procedure

Pieces of $B^+$ ribbon, approximately $5 \times 2 \times 0.04$ mm thick were supplied by Magnequench. Some of the ribbons analyzed by atom probe were melt spun at

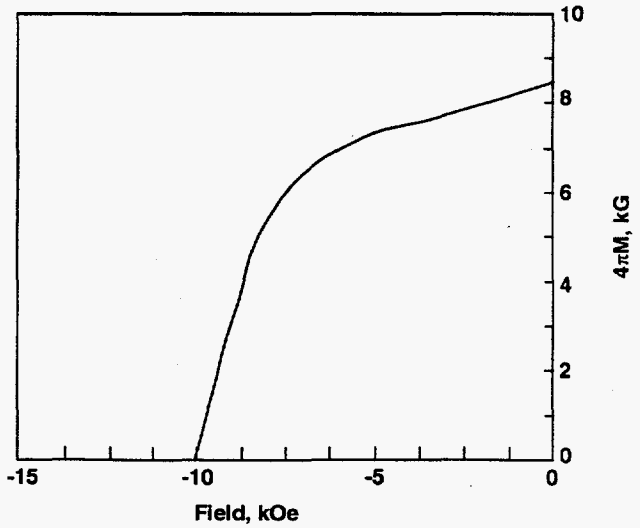


FIG. 1. BH curve for MQP-$B^+$

ORNL from an ingot supplied by Magnequench. These ribbons were $0.02 \times 0.4$ mm in cross section and made specimen preparation for the atom probe easier. The nominal composition of the $B^+$ ribbons was Fe-5 Co-0.9 B-28-total rare earth (wt.%). Specimens for TEM were made by ion milling in both the normal plan view orientation and in the cross section orientation. The plan view (top view) specimens that were made by back thinning to either the wheel side or the free side did not work due to the surface roughness. Cross section specimens (side view) were made by the usual techniques involving sandwiching the ribbons between layers of copper sheet, cutting out and mechanically thinning 3 mm disks following by mechanical dimpling and ion milling. Specimens for the atom probe were made following usual techniques in a 5% perchloric-acetic acid mixture. The analysis was done in ORNL's energy-compensated atom probe at a specimen temperature of 50 K and a pulse fraction of 15%. Specimens for AES were introduced into the high vacuum system and fractured under UHV conditions inside the PHI model 590 Scanning Auger Microprobe spectrometer immediately prior to analysis. Analysis was done at 5 keV and a current of ~140 nA. The data were collected in a voltage to frequency conversion mode.

## Results

SEM, Fig. 2 , and TEM, Fig. 3, images showed similar grain sizes and shapes throughout the thickness of the ribbon. The SEM images showed a recently fractured edge. The grain size was uniform throughout the thickness of the specimen. TEM images also showed an isotropic structure with similar grain sizes throughout the ribbon. Figures 3a,b, and c show cross section views (sideways) while (d) is a plan view, (looking down on the ribbon).

Preliminary results from the atom probe analysis of ribbon that was melt spun at ORNL showed compositions very close to the compositional analysis of the starting ingot, see Table 2. For this analysis, 30,000 ions were collected essentially from a cylinder of material approximately 2 nm in diam and 500 nm tall. Analysis of the MQI-$B^+$ powder gave similar results. Both analysis showed higher than expected carbon levels. Due to the low symmetry-large unit cell structure, FIM images are more complex than typical metals making identification of grain boundaries and grain boundary phases more difficult (Fig, 5), Within the composition profiles, see Fig. 4, fluctuations of Nd-Fe ratio were observed. One shown in Fig. 4 reached nearly 35% Nd. However, as a thin grain boundary phase sweeps past the probe hole, the atom probe analyzes both the potential grain boundary phase and some matrix. A statistical deconvolution is underway to separate out a potential grain boundary phase.

AES analysis was performed because it is a relatively easy technique for

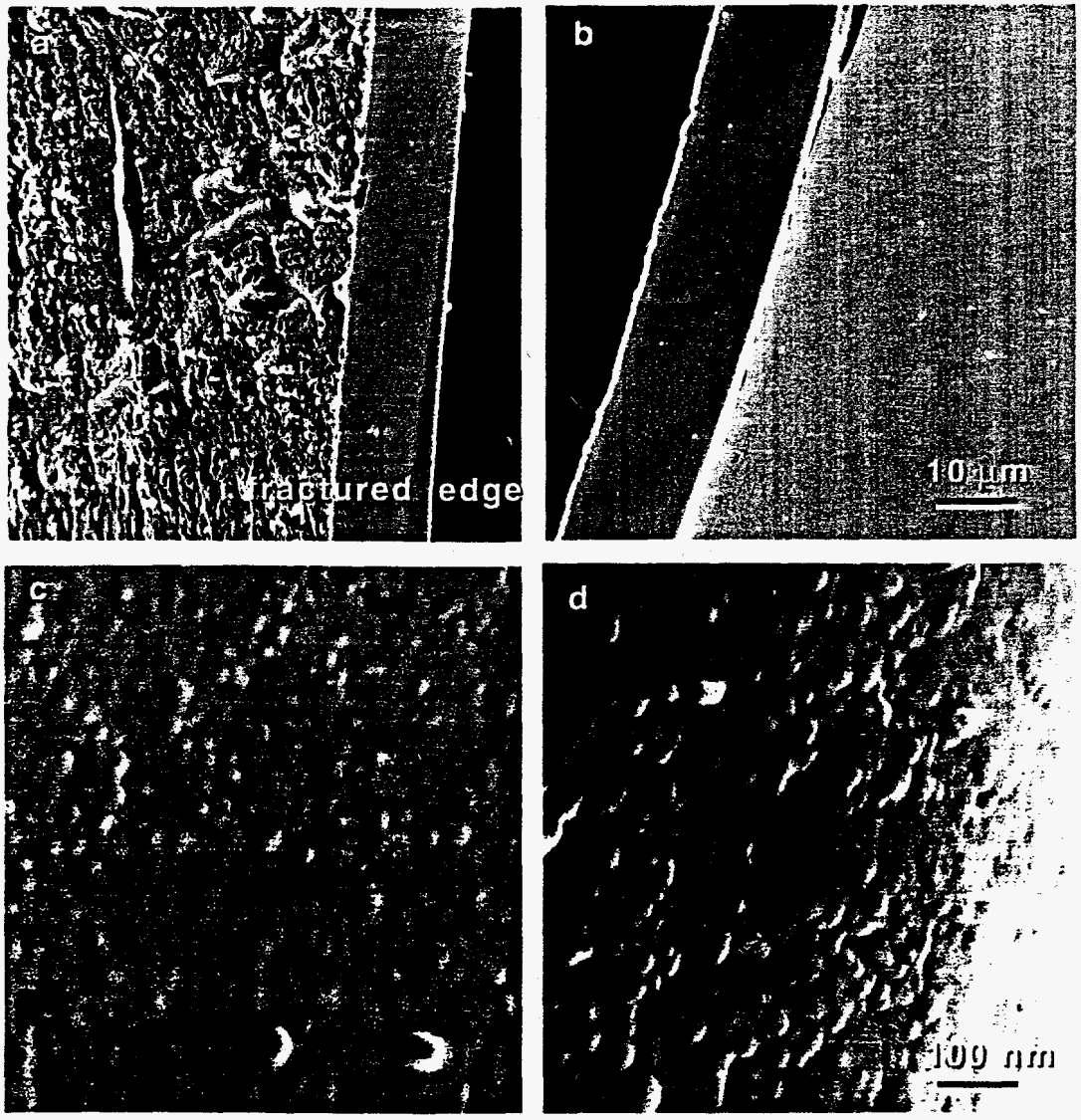


FIG. 2. SEM micrographs of melt spun ribbon, MQI-B+. (a) and (b) show rough and smooth (wheel) sides, respectively, while (c) is a fractured edge near the rough side and (d) is a fractured edge from near the wheel side.

accurately depth profiling an area. Previous results by AES (3) have shown that the fracture surfaces of MQ2 magnets are indeed intergranular with approximately a 1 nm thick layer of the expected 70Nd-30Fe phase present over most of the area of the fracture surface. Specimens of the ribbon were mounted in a similar way in the AES and were broken in the analysis chamber. Analysis of the ribbon also showed a similar neodymium enrichment at the surface. Figure 6 shows plots as a function of depth for Nd, Fe, B, and Co. After an analysis was performed, the surface was

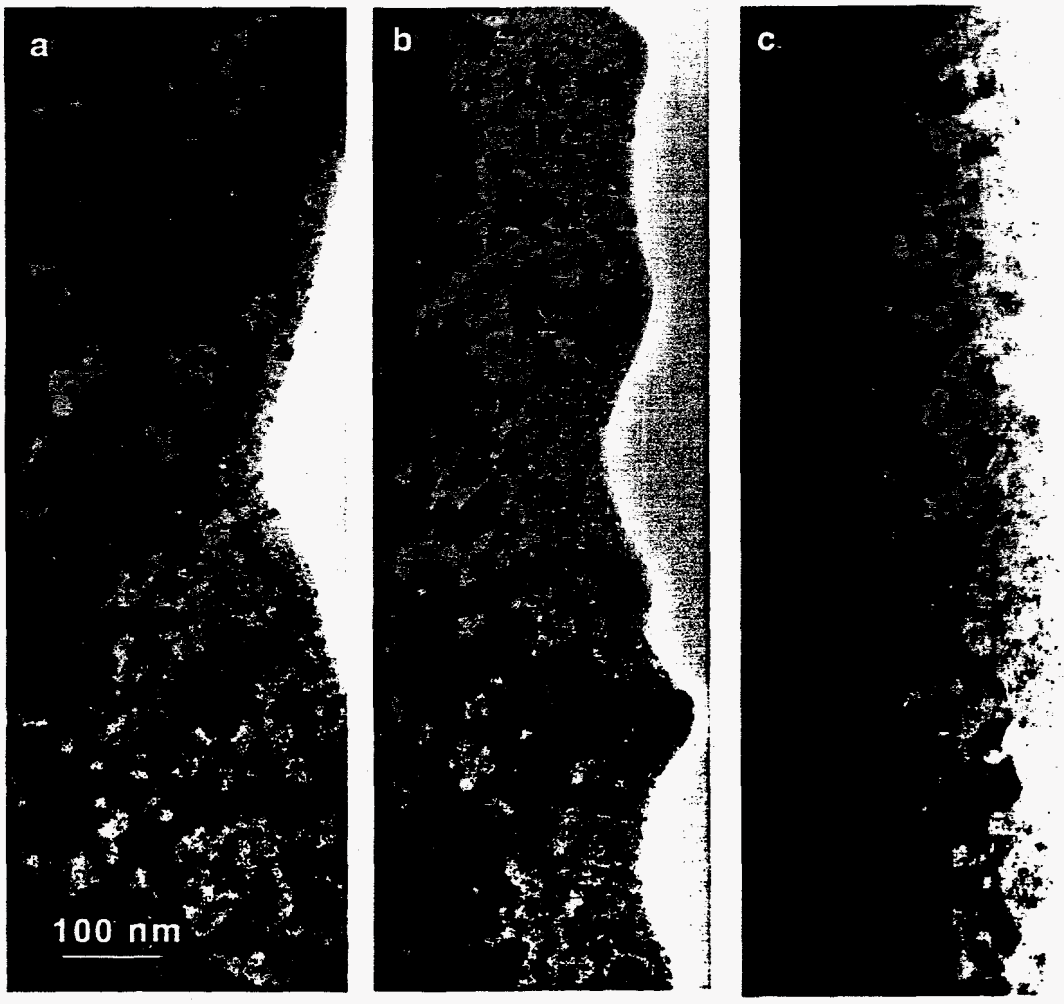



FIG. 3. TEM micrographs of MQI-$B^+$ powder showing uniformity of grain size through the thickness of the melt spun ribbon. Cross section images are of near one surface (a), near the middle (b) and near the other surface (c). (d) is a plan view from near the middle of the ribbon. All images are at the same magnification.

TABLE 2. Atom probe analysis of grain interiors (at.%)

| | MQI-B⁺ Powder | | ORNL melt spinning | |
|---|---|---|---|---|
| | Atom Probe | nominal | Atom Probe | Original ingot |
| Fe | 75.3±0.5 | 76.6 | 77.5±0.2 | 77.3 |
| Nd* | 12.9±0.4 | 12.6 | 11.2±0.2 | 13.6 |
| B | 5.2±0.2 | 5.5 | 6.6±0.14 | 6.1 |
| Co | 5.5±0.2 | 5.4 | 3.3±0.1 | 2.7 |
| C | 1.2±0.1 | - | 0.5±0.04 | NA |
| Al | 0.14±0.04 | - | 0.3±0.03 | 0.27 |
| Si | 0.11±0.04 | - | 0.6±0.04 | NA |
| Mn | 0 | - | 0 | 0.04 |
| Ga | 0 | - | 0 | 0.04 |

*Nd analysis includes other REs, NA- not analyzed, compositions in at.%

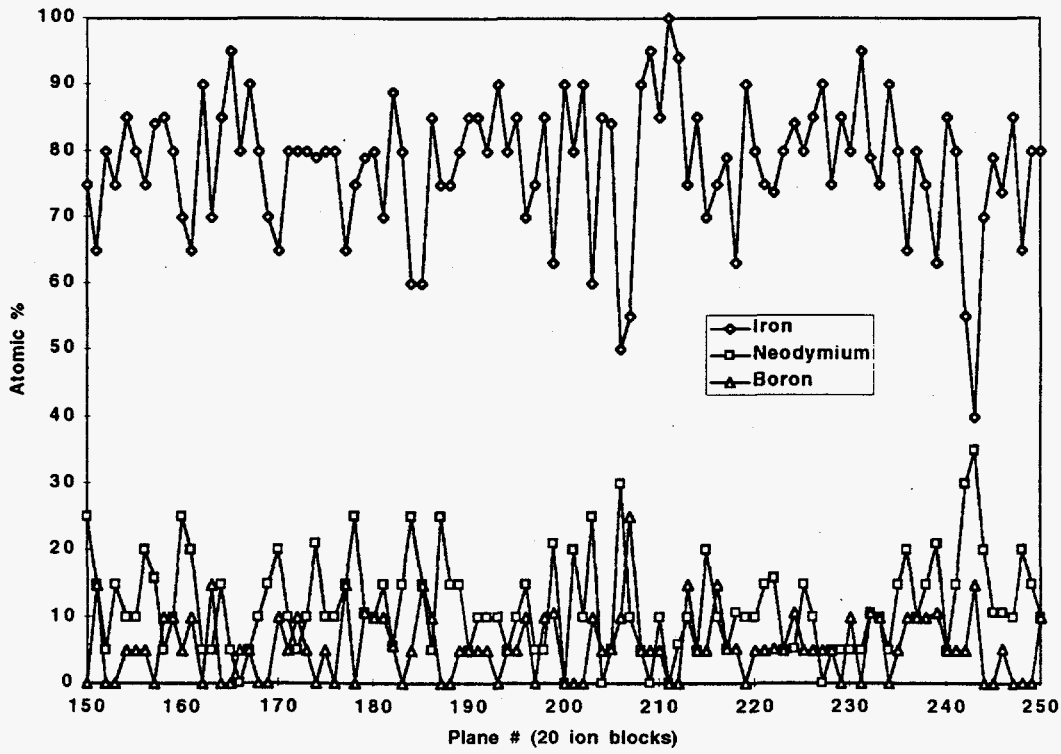


FIG. 4. Composition profile made by APFIM on a B⁺ ribbon through a probe hole with a diameter of approximately 20 nm.

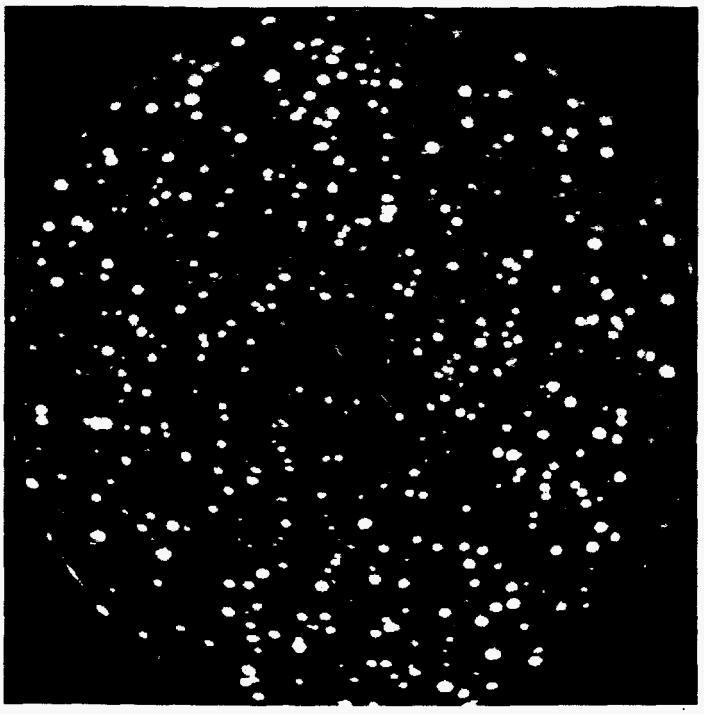

FIG. 5. APFIM image of $Nd_2Fe_{14}B$ melt spun ribbon. Due to the low symmetry and large unit cell, distinct rings and layers are absent.

subjected to an argon ion sputtering. The sputtering rate was approximately 1 nm per minute. The results here indicate that a fracture surface enrichment similar to that of bulk MQ2 magnets was present in the ribbon. Because some preferential sputtering artifacts are possible, an analysis of a cleavage face from a single crystal is planned to provide a good comparison.

## Conclusions

The new $B^+$ ribbons showed a uniform grain size and shape distribution through the thickness of the melt spun ribbon. Grain sizes ranged from 20 to 40 nm. AES showed neodymium enrichment on a fracture surface and corresponding iron and boron depletion suggesting that the eutectic 70Nd-30Fe phase is present with a thickness of approximately 1 nm. Atom probe composition analysis of grain interiors gave results very close to the nominal composition and some preliminary evidence of a grain boundary phase.

Acknowledgements

This research was sponsored by the U.S. Department of Energy, Office of Energy Research by the Laboratory Technology Research Program and by the Division of Materials Sciences, through the Center of Excellence for Synthesis and Processing of Advanced Materials under contract DE-AC05-96OR22464 with Oak Ridge National Laboratory managed by Lockheed Martin Energy Research Corp.

References

1. J. J. Croat, "Current Status and Future Outlook for Bonded Neodymium Permanent Magnets", *J. Appl. Phys.*, **81**(8)(1997)4804.
2. V. Panchanathan, "New High Performance Bonded Nd-Fe-B Permanent Magnets", *Proc. EIC/ EMCW Conf.*, (1997)375.
3. J. A. Horton, L. Heatherly, E., D. Specht, D. Li, J. W. Herchenroeder, and P. C. Canfield, "Brittle Fracture in $Nd_2Fe_{14}B$ Intermetallic Magnets" to be published Third Pacific Rim International Conf. on Advanced Materials and Processing (pub. by TMS) July 1998.
4. A. Hutten and P. Haasen, "Constitution of Melt-Spun NdFeB-Magnets Studied by Analytical Field Ion Microscopy", *Acta Met.* **39** (1991)1-11.

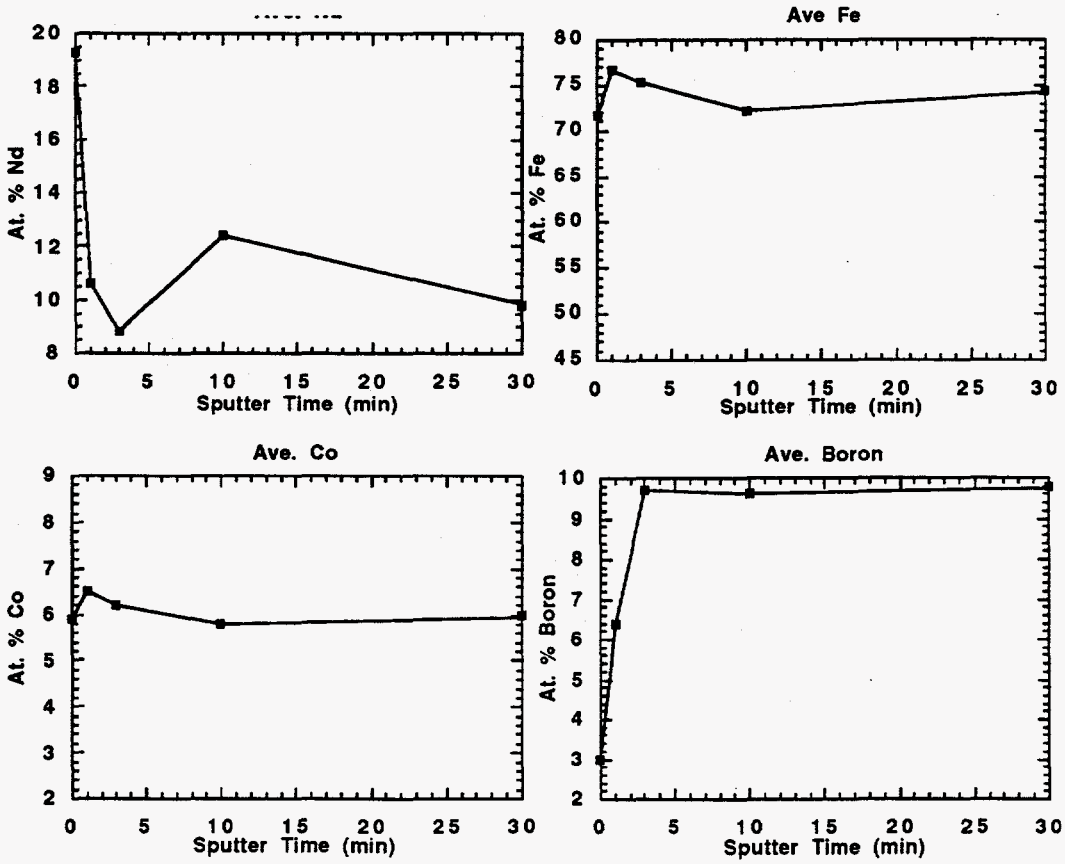


FIG. 6. AES spectra for Nd, Fe, Co, and B for a specimen of $B^+$ powder fractured in the analysis chamber. The argon ion sputtering rate was approximately 1 nm per minute.